Published in final edited form as:
J Cell Physiol. 2012 February ; 227(2): 534–549. doi:10.1002/jcp.22744.

Endothelial Cell Microparticles Act As Centers of Matrix Metalloproteinsase-2 (MMP-2) Activation and Vascular Matrix Remodeling

Thomas P. Lozito[1,2] and **Rocky S. Tuan**[1,2]

[1] Cartilage Biology and Orthopaedics Branch, National Institute of Arthritis and Musculoskeletal and Skin Diseases, National Institutes of Health, Department of Health and Human Services, Bethesda, MD 20892, USA

[2] Center for Cellular and Molecular Engineering, Department of Orthopaedic Surgery, University of Pittsburgh School of Medicine, Pittsburgh, PA 15219, USA

Abstract

Endothelial cell derived microparticles (MPs) are small membrane vesicles associated with various vascular pathologies. Here we investigated the role of MPs in matrix remodeling by analyzing their interactions with the extracellular matrix. MPs were shown to bind preferentially to surfaces coated with matrix molecules, and MPs bound fibronectin via integrin α_V. MPs isolated from endothelial cell-conditioned medium (Sup) were significantly enriched for matrix-altering proteases, including matrix metalloproteinases (MMPs). MPs lacked the MMP-inhibitors TIMP-1 and TIMP-2 found in the Sup and, while Sup strongly inhibited MMP activities, MPs did not. In fact, MPs were shown to bind and activate both endogenous and exogenous proMMP-2. Taken together, these results indicate that MPs interact with extracellular matrices, where they localize and activate MMP-2 to modify the surrounding matrix molecules. These findings provide insights into the cellular mechanisms of vascular matrix remodeling and identify new targets of vascular pathologies.

Keywords

microparticles; extracellular matrix; endothelium; matrix metalloprotease (MMP); tissue inhibitors of metalloprotease (TIMP)

INTRODUCTION

Microparticles are small (diameter < 1.0 μm) secreted vesicles released through an exocytotic budding process (Combes et al., 1999, Diamant et al., 2004). Produced by almost every cell type, microparticles contain both cytoplasmic components and membrane-associated elements of their parent cells (Combes et al., 1999, Freyssinet, 2003). The majority of microparticles in human blood are derived from platelets, with lower numbers originating from erythrocytes, granulocytes, monocytes, lymphocytes, and endothelial cells (ECs) (Diamant et al., 2004). MPs have proved to be of clinical relevance, and many disease states are associated with vascular microparticles, which are often discussed in terms of their procoagulant activity due to their catalysis of thrombin production (Diamant et al., 2004). Elevated levels of microparticles in blood increase the risk of thromboembolic

Address correspondence to: Rocky S. Tuan, Center for Cellular and Molecular Engineering, Department of Orthopaedic Surgery, 450 Technology Drive, Room 221, Pittsburgh, PA 15219. Fax: 412-624-5544; rst13@pitt.edu.

complications, and rare instances where patients have too few microparticles are met with increased bleeding (Diamant et al., 2004).

We are interested in the role of microparticles in the regulation of perivascular niche, and this study focuses on microparticles produced by ECs, the primary cell type of the vascular environment. We specifically focused on microparticles produced by microvascular ECs (microECs). MicroECs make up the microcirculation, including capillaries, and have been shown to interact with pericytic mesenchymal stem cells (MSCs) (Shi and Gronthos, 2003). Microparticles are released by unstimulated ECs and are detectable in the plasma of healthy humans (Combes et al., 1999). However, microparticles are found in significantly elevated numbers in patients presenting thrombic risk factors, such as lupus anticoagulant. These levels were not changed by medications (Combes et al., 1999). Increased numbers of microparticles were also reported for acute coronary syndromes, congestive heart failure, thrombotic thromobocytopenic purpura, multiple sclerosis, type I diabetes mellitus, and severe hypertension (Abid Hussein et al., 2003, Berckmans et al., 2001, Diamant et al., 2004, Forman et al., 1989, Jimenez et al., 2001, Mallat et al., 2000, Minagar et al., 2001). Decreased microparticle levels were reported in patients with sepsis and multiorgan failure (Diamant et al., 2004). In vitro, microparticle-production has been induced by a variety of factors, including complement proteins C5b-9, thrombin, and calcium ionophore (Combes et al., 1999, Hamilton et al., 1990).

Matrix-degrading properties have been associated with microparticles. Microparticles produced by cells of the skeletal system, e.g., hypertrophic chondrocytes of the endochondral growth plate, associate with matrix (Anderson, 2003). EC microparticles serve as centers of plasmin localization and activation, and matrix metalloproteinase-2, -9, and -14 (MMP-2, MMP-9, and MMP-14) activities have been associated with microparticles produces by cell types other than ECs (Lacroix et al., 2007). For example, microparticles shed by human breast carcinoma cells express MMP-2 and MMP-9 (Dolo et al., 1994). The few studies that were specific for EC microparticles and MMP-2, MMP-9, and MMP-14 considered microparticles produced by macrovascular ECs (macroECs) (Taraboletti et al., 2002). On the other hand, microEC microparticles have not been previously considered in terms of matrix interactions or MMP activity and activation.

The goal of this study was to characterize the possible role of microEC microparticles in the regulation of the perivascular proteolytic environment. In this manuscript, microparticles derived from microECs are referred to as ‘MPs’. Our first aim was to investigate the interaction between MPs and extracellular matrix molecules. Our second aim involved characterizing the endogenous protease activities associated with MPs. Finally, our third aim considered the role of MPs in MMP regulation and activation.

MATERIALS AND METHODS

Cell Culture

The microvascular endothelial cell (microEC) line HMEC-1 (obtained from Drs. Ades, Lawley, and Candal, Center for Disease Control) was cultured in endothelial cell (EC) medium (EGM-2-MV medium (Cambrex)). Human mesenchymal stem cells (MSCs) isolated from hip bone marrow provided by Dr. Paul Manner (IRB approved, University of Washington) as tissue culture plastic adherent cell populations were expanded in MSC medium (high-glucose DMEM containing 10% fetal bovine serum (FBS) and 1% penicillin-streptomyocin) and passaged at 70–80% confluency. All experiments were performed with passage 3–5 MSCs. Serum-free (SF) culture conditions involved replacement of serum with insulin-transferrin-selenium-x. Phenol red-free (PF) culture conditions involved replacement of basal media with phenol red-free Medium 199 (Invitrogen).

Cytokine and Hypoxia Treatment

Cell cultures were washed once with HBSS and fed SF PF medium. IL-1β and TNF-α groups were supplemented with 10 ng/ml rhIL-1β (Chemicon) or 10 ng/ml rhTNF-α (Chemicon), respectively. Control, IL-1β, and TNF-α groups were cultured for 24 hours at 37°C under normoxic conditions (20% O_2), while hypoxia groups were cultured under hypoxic conditions (2% O_2).

DiO-Labeled MP Production

MicroECs to be labeled with DiO (Invitrogen) were released by trypsinization and pelleted by centrifugation (5 min at 134.16 g). The supernatant was aspirated, and the cell pellets were resuspended at 1×10^6 cells/ml in EC basal medium. DiO solution was added (5μl per ml of cell suspension), and cells were labeled with gentle agitation for 20 minutes at 37°C. The cell suspensions were pelleted (5 min at 135×g), and excess DiO was removed by aspirating the supernatants. The cell pellets were washed 3 times with full EC medium. After the final wash, the microEC pellets were resuspended in EC medium and plated for the isolation of DiO-labeled MPs (see Microparticle Isolation section).

Microparticle Isolation

MicroECs were seeded at 1.0×10^4 – 1.25×10^4 cells/cm^2 in 150 cm^2 dishes and cultured until sub-confluent (typically 3 days) in full EC medium. Following HBSS washes, the cultures were fed with SF PF EC medium (15 ml per dish) for 24 hours. MP-containing medium was collected and cleared of cellular debris by centrifugation at 600×g and again at 1500×g, each for 15 min at 4°C. The clarified medium was ultracentrifuged at 100,000×g for 2 hrs at 4°C in a Beckman XL-70 Ultracentrifuge (SW40Ti rotor). (Note: Depending on the study, clarified medium was incubated with 0.5 ng//ml FITC-labeled fibronectin and/or EDTA (0.0 – 10.0 mM), GRGDS (Sigma) (2.5 mM), or GRADS (Sigma) (2.5 mM) for 1 hour prior to ultracentrifugation). The resultant pellets were resuspended in PBS and are referred to here as microparticles (MPs). The ultracentrifugation supernatants were concentrated using spin columns (Amicon Ultra-15 3 kDa NMWL, Fisher). The resulting concentrated ultracentrifugation supernatants are referred to here as EC Supernatant (Sup). MP and Sup samples were quantified for protein content using the BCA Protein Assay Kit (Pierce) and stored at −80°C. *Electron Microscopy* - MPs were visualized using protocols adapted from Dolo et al., 1994. Ultracentrifugation pellets resuspended in PBS were applied to collodion-coated grids, negatively stained with 1% phosphotungstic acid, pH 7.0, and observed with transmission electron microscopy (JEM-1011 Electron Microscope). Sizing of MPs were carried out by measuring the dimensions of 100 randomly selected MPs in the electron micrographs, and the data was analyzed with NIH ImageJ using the Particle Analysis function.

MicroEC Total Protein Collection

MicroECs were washed twice with ice-cold PBS before being scraped into PBS and spun at 840×g for 5 min. The pelleted cells were extracted in 0.25 ml of Total Protein Extraction Buffer (Millipore), and cell debris removed by centrifugation at 12,851×g for 20 min. The protein-containing supernatants were collected and are referred to here as microEC total protein (TP).

Western Blotting

Protein samples (10 μg) were subjected to reducing SDS-PAGE and transferred to low-fluorescence background polyvinylidene fluoride membranes (Millipore). Membranes were blocked in 3% milk in TBS-T (.25% Tween-20 in TBS) for 1 hour and probed overnight at 4°C with various antibodies (N-Cadherin, Abcam; VE-Cadherin, R&D; E-cadherin, Abcam;

integrin α_V, R&D; integrin $\alpha_V\beta_3$, R&D; actin, Santa Cruz; GAPDH, Millipore; fibronectin, R&D; MMP-2, Chemicon; MMP-9, Chemicon; MMP-1, Abcam; MMP-13, Abcam; MMP-7, Abcam; plasminogen, Abcam; MMP-14, Santa Cruz; active MMP-14, Chemicon; MMP-15, Abcam; MMP-16, Abcam; TIMP-1, R&D; TIMP-2, R&D; TIMP-4, Chemicon; pan-cadherin, Abcam) in 1% milk/TBS-T. (Note: For antibody-validation studies involving neutralization peptides, antibodies were incubated with 5-fold excesses of blocking peptides (Santa Cruz) in 500 μl of PBS overnight at 4° C.) After washing, membranes were incubated for 1 hr with the appropriate AlexaFluor 488-conjugated secondary antibody diluted 1:2000 in 1% milk/TBS-T. Bands were visualized with a Typhoon 9410 Variable Model Imager (Molecular Dynamics) using a 532 nm green laser and a 526 nm SP filter. Each blot was repeated at least in duplicate, and representative scans are presented.

MSC-Conditioned Medium (MSC-CM) Collection

MSCs were cultured in SF PF medium for 24 hours, and the conditioned medium was collected and centrifuged at 838.5 g for 10 min at 4°C to remove cellular debris. The cleared samples were concentrated using spin columns (Fisher). The resulting concentrated medium is referred to here as MSC-CM.

Enzyme-linked immunosorbent assays (ELISAs)

TP, MP, and Sup protein samples collected in PBS (50 μg total protein per sample) were analyzed by fibronectin (Millipore) and MMP-2 (R&D) ELISAs following the manufacturers' instructions. The fibronectin ELISA is a competitive inhibition ELISA, while the MMP-2 ELISA employs the quantitative sandwich enzyme immunoassay technique.

MP Adhesion Assay

Coating solutions (50 μl) of extracellular matrix molecules, including fibronectin (0.032 mg/ml, Millipore), gelatin (2%, Sigma), Matrigel (1:10, BD), and bovine serum albumin (BSA, 2%, Sigma) as control, were incubated overnight in black 96-well plates at room temperature and washed with DPBS (+$CaCl_2$, +$MgCl_2$) (Gibco). 50 μl of DiO-labeled MPs (1 μg/μl MP protein) (see DiO-Labeled MP Production) were added to one set of Matrigel-, fibronectin-, gelatin- and BSA-coated wells and incubated for 4 hours at 37°C. The *total* relative number of vesicles for each well was determined by fluorescence photometry (Ex/Em = 485/535). Next the wells were washed once with DPBS and replaced with fresh DPBS, and the numbers of *bound* MPs were measured via photometry. Fluorescence measurements were related to MP protein amount via standard curves (see Supplemental Figure 1). The percentage of ECMPs bound by each type of surface was determined by relating the average number of bound ECMPs to the average total number of ECMPs.

Labeling of Extracellular Matrix Molecules with FITC

Human fibronectin (Sigma) was diluted to 0.5 mg/ml of 40 mM NaCl/170 mM $Na_2B_4O_7$ (pH 9.3) buffer and dialyzed against 0.03 mg/ml FITC in 50 mM $Na_2B_4O_7$ (pH 9.3) for 90 minutes. The labeled proteins were then dialyzed extensively against PBS to remove unreacted FITC.

Identification of Fibronectin Receptors with the Biotin Transfer Reagent Sulfo-SBED

Sulfo-SBED (sulfo-N-hydroxysuccinimidyl-2-(6-[biotinamido]-2-(p-azido benzamido)-hexanoamido) ethyl-1,3′-dithioproprionate) (Pierce) was diluted to 100 μg/ml in dimethyl sulfoxide (DMSO) and diluted 1:500 in 1 mg/ml human fibronectin (Sigma) and allowed to react for 2 hours at 4°C with agitation. Unreacted sulfo-SBED was removed by dialysis against 50 mM HEPES/150 mM NaCl (pH 7.3) overnight at 4°C. The sulfo-SBED-labeled

fibronectin was diluted 1:10 in 1 mg/ml samples of MP proteins. The reaction mixes were rotated for 60 min at room temperature and crosslinked with a Spectroline SB-100P UV lamp (365 nm) positioned 8 cm away for 5 min.

Monomeric Avidin Purification of Sulfo-SBED-Labeled Molecules

Monomeric avidin-conjugated resin (Pierce) was loaded into micro spin-columns (Pierce) and equilibrated according to the manufacture's instructions. Samples were diluted to 300 μl in PBS, added to the resin, and incubated for 1 hr at room temperature. After centrifugation at 1000g for 1 min, the avidin resin (containing the bound biotinylated protein complexes) was washed seven times in TBS-B (1x TBS, 5mM $CaCl_2$, 0.02% v/v Brij-35), incubated with 100 μl Biotin Blocking and Elution Buffer (Pierce) for 30–60 minutes, and the fractionated protein was isolated following centrifugation of the resin at 1000g for 2 min.

Zymography

Gelatin zymography was performed using 8% Tris-glycine SDS-polyacrylamide gels containing 1 mg/ml gelatin. Fibrin zymography employed 12% gels containing 0.5 NIH unit/ml thrombin and 2.0 mg/ml fibrinogen. 15% gels containing 2.5 mg/ml and 160 ng/ml MMP-9 were used for reverse zymography. 10 μg protein samples were mixed with zymogram sample buffer (BioRad) and separated with SDS-PAGE at 4°C. The gels were then equilibrated with zymogram renaturation buffer (BioRad) and incubated with zymogram development buffer (BioRad) overnight at 37°C. Bands were visualized by staining gels with Simply Blue Safe Stain (Invitrogen). At least 2 replicates were carried out for each sample analyzed by zymography, and representative scans are presented.

APMA-Treatment of Protein samples

Membrane, MP, and Sup protein samples were incubated with 1mMAmino-phenyl mercuric acetate (APMA) or vehicle control overnight at 37°C.

MMP activity assays

10 μg protein samples and vehicle controls were incubated with MMP Fluorogenic Substrate I (DabcylPlus-KPLA-Nva-D(EDANS)-AR-NH_2) (Anaspec), Substrate II (Dabcyl-γ-Abu-PQGL-E(EDANS)-AK-NH_2) (Anaspec), or Substrate III (QXL520-γ-Abu-PQGL-Dab(5-FAM)-AK-NH_2) (Anaspec) diluted 1:100 for 60 minutes. Assays involving Substrates I and II were measured for their fluorescence intensities at Ex/Em = 355/460 nm, while assays involving Substrate III was analyzed at Ex/Em = 485/520 nm. MMP activities were determined by subtracting the fluorescence measurement for a sample from that of the corresponding vehicle control.

MMP inhibitor assays

MMP-2, -9, -1, and -13 (Calbiochem) were activated with 1 mM APMA for 2–24 hours at 37°C. Samples and vehicle controls were prepared in two sets. Activated MMPs were added to one set of samples and blanks to 250 ng/ml. All samples and blanks were incubated at 37°C for 15 min. MMP Fluorogenic substrates I, II, or III were added 1:100 to inhibitor assays, and, following incubations for 1 hour at 37 C, fluorescence intensities were measured. Fold differences in MMP activity between samples combined with MMPs and corresponding vehicle controls combined with the same MMPs were determined.

MMP-2 Activation

Samples of MPs and EC Sup were diluted to 0.5 μg total protein per μl in MMP Buffer (50 mM Tris-HCl pH 7.5, 150 mM NaCl, 5 mM $CaCl_2$ 0.025% Brij 35) with or without 1x MSC-CM/vehicle control and incubated for 20 hrs at 37°C.

Statistics

Unless otherwise stated, each sample was analyzed over 5 experimental replicates. Results are expressed as the mean ± SD, and significant differences among experimental conditions were determined by two-tailed Student's t-tests for two-group comparisons or ANOVA followed by post-hoc analysis for multiple group comparisons. p values < 0.05 were considered significant. Experiments involving MSCs were repeated with cells derived from at least 3 patients. Results from the same representative patient are presented.

RESULTS

MPs are plasma membrane-derived vesicles that bind surfaces coated with matrix molecules

MP-isolation was validated by electron microscopy analysis of ultracentrifugation pellets produced from microEC-CM. The isolated MPs consisted of mostly sealed membranous vesicles ((Figure 1A) with an average diameter of 73.75 ± 36 nm (Figure 1B), consistent with the reported size for MPs and too small to be apoptotic bodies (Hristov et al., 2004). To confirm the plasma membrane origin of MPs, we tested for the transfer of DiO, a membrane fluorescent dye, from microECs to MPs via fluorescence photometry. Membrane extracts of the DiO-labeled microECs were analyzed as positive controls. The isolated MPs and membrane extracts were significantly enriched for fluorescence compared to EC-conditioned medium supernatant (Sup) fractions, indicating that DiO membrane-labeling of MPs was effective and specific (Figure 1C). Fluorescence measurements of MPs normalized to protein amount were comparable to those of microEC membrane extracts, further suggesting that MPs contained membrane components. The presence of plasma membrane-associated proteins in MPs was investigated (Figure 1D). Samples of microEC total protein and Sup fractions were included as positive and negative controls, respectively. MPs contained a subset of microEC surface proteins involved in cell-cell and cell-matrix interactions, including N-cadherin, VE-cadherin, and integrin α_V.

The effects of inflammatory cytokines and hypoxia on MP production were investigated (Figure 1E). MicroECs were exposed to IL-1β, TNF-α, or hypoxic conditions, and the production of MPs was assessed by means of DiO fluorescence labeling. Significantly higher fluorescence was found in the MP fractions isolated from ECs treated with IL-1β, TNF-α, and hypoxia than from ECs cultured under control conditions, suggesting that exposure to inflammatory cytokines and hypoxia increased the level of MP production by microECs.

DiO-labeled MPs bound surfaces coated with Matrigel, fibronectin, and gelatin, suggesting that MPs bind matrix molecules found in a wide variety of extracellular matrix molecules, including vascular matrix (Figure 1F). Furthermore, MPs produced in the presence of inflammatory cytokines or hypoxia exhibited enhanced matrix-binding properties (Figure 1G). MPs collected from DiO-labeled microECs treated with IL-1β, TNF-α, or hypoxia were incubated with fibronectin-coated surfaces, and the percentage of MP-binding normalized to the starting amounts of MPs used was measured for each condition. Higher levels of adherence to fibronectin were seen in MPs produced in the presence of IL-1β, TNF-α, or hypoxia compared to control conditions. Thus, simulated pathological conditions stimulated microECs to produce higher overall amounts of MPs that displayed inherently higher matrix-binding activity. The overall result is more MPs bound to the matrix under pathological conditions.

MPs bind endogenous fibronectin in an EDTA- and RGD-sensitive manner

Endogenous fibronectin secreted by microECs was found to co-precipitate with MPs during isolation by ELISA and western blot (Figure 2A and B, respectively). MicroEC-secretion of fibronectin and co-precipitation of fibronectin and MPs was not affected by IL-1β, TNF-α, or hypoxia. Similarly, cytokine- and hypoxia-treatment did not affect expression of integrin $\alpha_V\beta_3$ by microECs or MPs. To test the Ca^{2+}-dependence of interactions between MPs and endogenous fibronectin, MPs were precipitated in the presence of EDTA. Treatment with 5.0 and 10.0 mM EDTA reduced the amount of fibronectin co-precipitated with MPs (Figure 2C). EDTA treatment did not affect MP integrin α_V levels, indicating that EDTA directly affected binding interaction between fibronectin and MPS rather than altering the content of the matrix-binding molecules in MPs. To test whether the MP-fibronectin interactions involved integrins, MPs were precipitated in the presence of 2.5 mM of the peptide RGD, a competitive inhibitor of fibronectin-integrin binding, or the control peptide RAD (Figure 2D). The presence of RGD, but not RAD, interfered with co-precipitation of fibronectin with MPs. Again, neither RGD nor RAD affected MP integrin α_V-expression, indicating that RGD-interference of fibronectin-binding by MPs was due to inhibition of integrin binding activity and not due to changes in integrin levels.

MPs bind exogenous fibronectin with integrin α_V

We next analyzed MP-binding to fibronectin using exogenous FITC-labeled fibronectin (Fn-FITC) in conjunction with fluorophotometric measurements and fluorescence scans of SDS-PAGE protein gels. Fn-FITC bands were detected in MP samples pre-incubated with 0.5 ng/ml Fn-FITC before ultracentrifugation, indicating that exogenous fibronectin co-precipitated with MPs (Figure 3A). In the controls, Fn-FITC incubated with MP-free EC Med did not precipitate, and fluorescent bands were not detected in MP samples incubated without Fn-FITC. Fn-FITC did not affect integrin α_V-expression in MPs, indicating direct interaction between MPs and exogenous fibronectin. These results were confirmed with fluorophotometric measurements; the MP fractions incubated with Fn-FITC displayed significantly higher fluorescence measurements than similar fractions from either Fn-FITC incubated without MPs or MPs incubated without Fn-FITC (Figure 3B). Fluorescence photometry measurements were converted to fibronectin amount with the use of standard curves (see Supplemental Figure 1). To determine whether interactions between exogenous fibronectin and MPs were Ca^{2+} and/or integrin-dependent, incubation was done in the presence of 10 mM EDTA or the peptides RAD or RGD (2.5 mM) (Figure 3C). EDTA and RGD interfered with the co-precipitation of Fn-FITC with MPs, while RAD did not. Again, treatment with neither EDTA nor RGD (or RAD) affected MP integrin α_V levels, indicating direct action on the interactions between exogenous fibronectin and MPs. Protein gel results were confirmed with photometry measurements; Fn-FITC incubated with MPs in the presence of EDTA or RGD exhibited significantly lower fluorescence measurements than untreated MPs or MPs incubated with RAD, respectively (Figure 3D).

Next we identified the specific MP proteins involved in binding exogenous fibronectin (fibronectin receptors) using the heterobifunctional crosslinker and biotin transfer reagent sulfo-SBED in a “bait and fish” scheme (Figure 3E). Exogenous fibronectin pre-labeled with the amine-reactive NHS-ester groups on one end of the sulfo-SBED molecules was incubated with MPs and UV-activated to covalently crosslink the aryl azide group on the other side of sulfo-SBED to the fibronectin receptors. Sulfo-SBED also includes a biotin group separated from the NHS-ester-terminal end by a cleavable disulfide spacer arm. Thus, when the MP/fibronectin samples were analyzed via SDS-PAGE under reducing conditions, the biotin group was transferred to the fibronectin receptor. Following transfer to PVDF membranes and probing with AlexaFluor 488-cogugated neutravidin, fibronectin receptors with molecular weights of 120 kDa were identified by fluorescent scanning (Figure 3F).

These same proteins were recognized in integrin α_V western blots, but not integrin α_1, α_3, α_4, α_5, α_6, α_{IIb}, β_1, β_3, or β_5 blots (data not shown), indicating that integrin α_V was a fibronectin receptor used by MPs to bind exogenous fibronectin. As controls, samples of sulfo-SBED-labeled-fibronectin were incubated with MPs in the presence of EDTA (10 mM), RAD (2.5 mM), or RGD (2.5 mM) and processed as described above. Fibronectin receptors were detected in samples incubated with RAD, but not in samples treated with EDTA or RGD. Treatment with neither EDTA, RGD, nor RAD affected MP integrin expression, suggesting that EDTA and RGD interfered with the transfer of biotin from fibronectin to the 120 kDa fibronectin receptor/integrin α_V and not with the integrin molecules or MPs themselves.

We confirmed integrin α_V as an MP fibronectin receptor with the use of monomeric avidin precipitation of sulfo-SBED-labeled fibronectin protein complexes (Figure 3G). MP samples incubated with sulfo-SBED-fibronectin were incubated with monomeric avidin resin following aryl azide crosslinking of fibronectin receptors. Monomeric avidin, with its lower biotin-binding affinity than native tetrameric avidin, allows for the recovery of biotinylated molecules using mild elution conditions. Western blot analysis of fibronectin receptor complexes purified from the avidin resin revealed high levels of integrin α_V which co-precipitated with fibronectin. As controls, integrin α_V was not detected in avidin-purified fibronectin samples alone, and avidin resins exhibited very low levels of nonspecific integrin α_V binding. These results confirm α_V as an MP-associated fibronectin receptor.

MMP and TIMP activities of MPs

Localization of secreted proteases to the MP or Sup fractions of microEC-CM was investigated by western blot analysis of MMP and plasminogen (Figure 4). To validate MMP bands in MP and Sup fractions, protein samples were incubated with APMA or vehicle control overnight at 37°C (Figure 4A). In this way, MMPs activated by APMA treatment were detected as shifts in band size corresponding to their pro- and active forms. MPs were shown to express MMP-2, -13, -7, and -1. MMP-13 and MMP-7 levels were undetectable in Sup samples. MP binding of endogenous MMP-2 was confirmed by ELISA (Figure 4B). The presence of plasminogen in MP and Sup was confirmed by fibrin zymography (Figure 4C). For membrane-type MMPs, microECs and MPs expressed MMP-14, -15, and -16 in both their respective latent and active forms (Figure 4D). (See Supplemental Figure 2 for validation of MMP-14, 15, and 16 antibodies.) Active MMP-14 bands in TP and MP samples were validated using anti-proMMP-14 antibodies. The Sup fraction of microEC-CM exhibited no detectable expression of any membrane-type MMP. Taken together, these results suggested that MPs were enriched in MMPs and other proteases, such as plasmin and membrane-type MMPs, known to be involved in MMP activation.

Localization of MMPs to microEC MPs was confirmed with MMP activity assays (Figure 5A). Fluorimetric MMP assays utilizing three different MMP substrates showed that MPs exhibited significantly higher MMP activities than Sup fractions of microEC-CM. (See Supplemental Figure 3 for validation of substrates in MMP activity assays.) MMP activities of MPs were comparable to those of microEC membrane extracts. Activation with APMA significantly increased MMP activity in membrane, MP, and Sup samples, but membrane and MP samples remained more MMP-active than Sup samples. MMP protein expression in MP, membrane, and Sup samples were validated with western blot (Figure 5B) and gelatin zymography (Figure 5C). MPs contained MMP-2, while membrane factions did not. MPs expressed active MMP-14, while both active and latent forms of MMP-14 were detected in membrane extracts. (Note: Membrane extraction methods were validated with western blots of membrane samples exhibiting enrichment for cadherins and deficiencies in cytoplasmic

proteins like GAPDH.) Taken together, these results suggest that MPs act as centers of MMP expression and activity.

The presence of TIMPs in MPs was assayed via reverse zymography and confirmed with western blots (Figure 6A). (See Supplemental Figure 4 for validation of reverse zymography). Reverse zymography involves several modifications to the traditional substrate zymography technique that allows for the detection of TIMPs rather than MMPs in protein samples (Oliver et al., 1997). Briefly, MMPs are included in the preparation of the substrate zymography gel. Protein samples are loaded into the gel and electrophoretically separated by size. The gels are then developed and stained with Coomassie Blue. In traditional substrate zymography, MMPs are visualized as bands of negative staining corresponding to regions of gel cleared of substrate protein. In reverse zymography gels, substrate protein is cleared by the MMPs included in the gel preparation throughout the gel except in areas corresponding to MMP inhibitors. Thus, TIMPs are visualized in reverse zymography gels as bands of positive staining of substrate protein. Unlike microEC Sup fractions, MPs did not contain TIMP-1 or TIMP-2, but instead high levels of TIMP-4. TIMP activities measured with MMP inhibitor assays showed that microEC Sup effectively inhibited exogenous, pre-activated MMPs-2, 9, 1, 13, and 14, while MPs exhibited significantly lower levels of MMP inhibition than Sup fractions and comparable levels to microEC membrane extracts despite the expression of TIMP-4 (Figure 6B). Given the reverse zymography results, these observations were likely due to the substantially lower levels of TIMP-1 and TIMP-2 associated with MPs.

To examine the influences of in vitro simulated pathological conditions, cells were exposed to the cytokines IL-1β and TNF-α and hypoxia and assayed for MMP/TIMP expression/activity (Figure 7). Cytokine and hypoxic conditions did not affect MMP-2 or MMP-1 localization to MPs (Figure 7A) or MP expression of active MMP-14 (Figure 7B). MPs also remained centers of MMP activity under simulated pathological conditions (Figure 7C). MPs maintained low levels of TIMP-1 and TIMP-2 and high levels of TIMP-4 despite the presence of inflammatory cytokines and hypoxia (Figure 7D), and microEC Sup showed significantly higher levels of MMP-inhibition than MPs under simulated pathological conditions (Figure 7E).

Modulation of MMPs by MPs

The presence of plasmin, MMP-1, and MMP-14, molecules known to have MMP-activating properties, prompted us to examine the effects of MPs on MMP activation. We first considered activation of endogenous MMPs. Inactive proMMP-2 was detected in MP and Sup fractions by gelatin zymography and western blot. Following incubation for 20 hours at 37°C, MPs, but not microEC Sup, exhibited active MMP-2 (Figure 8A). This activation was specific for MMP-2, as no changes in MMP-1 or MMP-13 were detected for either MP or Sup fractions. Activation of MMP-2 was confirmed with MMP activity assays, which showed significantly increased MMP activities in incubated MP samples compared to Sup fractions (Figure 8B). MP MMP-2 activation was also found to be time-dependent, with active MMP-2 only being detected after at least 12 hours of incubation (Figure 8C). Taken together, these results suggested that MPs activated MMP-2, a property not shared by the local environment.

We next investigated the mechanism by which MPs activated endogenous MMP-2 with the use of various protease inhibitors: 10 mM EDTA, an inhibitor of MMPs; 10 mM 6-aminocaproic acid (6-ACA), a plasmin inhibitor; 20 μM GM6001, a global MMP inhibitor that interferes with MMP-14 activation of MMP-2; 2 μM MMP-2/9 Inhibitor IV, an inhibitor specific for MMP-2 and -9 that does not interfere with MMP-14 activation of MMP-2 at the concentrations used (Ikejiri et al., 2005); 1–10 nM TIMP-1, which is reported

to preferentially inhibit MMP-1 (Brew et al., 2000, Visse and Nagase, 2003); and 1–10 nM TIMP-2, which inhibits MMP-14 (Brew et al., 2000, Visse and Nagase, 2003) (Figure 8D). The effectiveness of these inhibitors and concentrations on MMP-14 and MMP-1 were validated with MMP-14 and MMP-1 activity assays (Figure 8E). EDTA and GM6001 inhibited both MMP-14 and MMP-1. Neither MMP-1 nor MMP-14 was inhibited by 6-ACA or MMP-2/9 inhibitor IV. MMP-1, but nor MMP-14, was inhibited by TIMP-1, while TIMP-2 inhibited both MMP-1 and MMP-14. As described above, MP samples incubated at 37°C under control conditions for 20 hours results in active MMP-2. MMP-2 activation was inhibited by EDTA, GM6001, and TIMP-2 and was unaffected by 6-ACA, MMP-2/9 inhibitor IV, and TIMP-1. These results closely match those of the MMP-14 inhibitor assays, suggesting that membrane-type MMPs were responsible for MP activation of MMP-2.

We also examined the influence of pro-inflammatory cytokines and hypoxia on the abilities of MPs to activate endogenous MMP-2. While only proMMP-2 was present in the MPs and Sup produced in the presence of IL-1β, TNF-α, and hypoxia, all MP samples incubated at 37°C for 20 hours showed active MMP-2, whereas EC Sup samples contained only inactive proMMP-2 regardless of treatment or time point (Figure 8F). These results were confirmed with MMP-2 activity assays, suggesting that MPs remain centers of MMP-2 activation despite simulated pathological conditions (Figure 8G).

MPs bind and activate exogenous MMP-2

Having shown that MPs co-precipitated with endogenous MMP-2, we next tested the abilities of MPs to bind exogenous MMP-2. MSCs were used as the source of MMP-2. MSCs have been shown to be perivascular (Crisan et al., 2008), and their interaction with microECs and MPs is physiologically relevant. We and others have previously shown that MSCs secrete high levels of proMMP-2 (Lozito and Tuan, 2010, Ries et al., 2007). Higher levels of proMMP-2 were detected in MPs incubated with MSC-CM prior to isolation than in MPs incubated with vehicle controls (Figure 9A). MSC-CM MMP-2 did not precipitate in the absence of MPs, indicating that co-precipitation of exogenous MMP-2 with MPs depended on binding interactions. These results were confirmed with MMP activity assays; MPs incubated with MSC-CM exhibited significantly higher MMP activities than either MSC-CM incubated without MPs or MPs incubated without MSC-CM (Figure 9B).

MPs and microEC Sup fractions were also tested for their abilities to activate exogenous MMP-2 by incubating MSC-CM with MPs or Sup for 20 hours. Active MMP-2 was detected in MSC-CM samples incubated with MP but not with Sup (Figure 9C), while MP samples incubated alone without MSC-CM contained comparatively undetectable MMP-2 levels (data not shown). MSC-CM samples incubated with MPs also exhibited significantly increased levels of MMP activity compared to MSC-CM incubated with EC sup (Figure 9D). Finally, the time dependence of MP-mediated activation of MSC-CM MMP-2 was also confirmed (Figure 9E).These results suggested that MPs not only activated MMP-2 found in MSC-CM, but also created an environment where activated MMP-2 cleaved substrates.

MPs Bind and Degrade Fibronectin

That MPs contained MMPs and were able to bind to matrix molecules such as fibronectin prompted us to examine MP-modification of bound matrix molecules. First we studied degradation of matrix molecules by MPs. Samples of Fn-FITC co-precipitated with MP were incubated 0 or 3 days and analyzed with fluorescence scans following SDS-PAGE. MP-bound Fn-FITC, but not Fn-FITC incubated with the Sup fraction, was degraded following incubation, as evidenced by the decrease in fluorescence associated with the 250 kDa Fn-FITC bands (Figure 10A). The involvement of MMPs in MP-degradation of bound

fibronectin was shown by the inhibitory effects of 20 mM GM6001 (Figure 10B). MMP-mediated Fn-FITC degradation also depended on binding interactions between MPs and fibronectin. MPs incubated with Fn-FITC for 3 days in the presence of 10 mM EDTA or 2.5 mM RGD failed to degrade Fn-FITC compared to controls (0 mM EDTA, 2.5 mM RAD) (Figure 10C).

DISCUSSION

To study regulation of the perivascular niche, we have chosen to focus on microparticles produced by microECs rather than macroECs using the well characterized microEC line HMEC-1 (Ades et al., 1992, Xu et al., 1994). Originating from the microcirculation, the dominant feature of the vasculature, where they interact with pericytes and MSCs (Lacroix et al., 2007), microECs are particularly relevant in studies of the perivascular environment. Furthermore, compared to macroEC, microECs exhibit superior retention of phenotype and more physiological responses to simulated pathologic conditions under in vitro culture conditions (Madri et al., 1991). Despite these reports, the majority of previous microparticle studies, and all those that considered MMP activity, have employed macroECs (Diamant et al., 2004, Lacroix et al., 2007, Taraboletti et al., 2002).

Our first aim was to determine whether microEC MPs associated with extracellular matrix. The MPs used in this study expressed molecules such as integrin $\alpha_V\beta_3$ that mediate interactions with matrix molecules. Other studies have shown that macroEC microparticles contain integrins, speculating that they might associate with matrix (Combes et al., 1999, Taraboletti et al., 2002). Our study is the first to directly measure the binding of microEC MPs to matrix molecules. We began by characterizing the binding interactions between MPs and fibronectin. MPs bound to both endogenous and exogenous fibronectin in a Ca^{2+}-dependent, RGD-sensitive manner. In the case of exogenous fibronectin, integrin α_V was identified as the primary fibronectin receptor with the use of the heterobifunctional crosslinker sulfo-SBED, the first instance of such a strategy being used to investigate MP interactions.

Next we developed a fluorescence-based assay to analyze MP production and behavior via transfer of fluorescent membrane dyes from the parent cells. Previous methods of fluorescently-tagging MPs have been predominantly based on annexin V-binding (Diamant et al., 2004). However, annexin V only binds MPs displaying the phospholipid phosphatidylserine (PS) on their outer surfaces, a trait shared with apoptotic bodies. In comparison, labeling microECs with membrane dyes, which we showed to be efficiently transferred to secreted MPs, offers more direct, uniform measurements of the entire MP-population.

While molecular binding is an important means by which MPs may interact with their matrix environment, we were particularly interested in whether MPs could alter and regulate this environment and focused on their contribution to the proteolytic microenvironment. Our second aim was to characterize the endogenous MMP-activity of MPs. MPs were shown to express both soluble and membrane-type MMPs, molecules known to be of critical importance in regulating matrix. and exhibited elevated MMP activity levels. These MP MMP activities were not shared with the remainder of factors secreted by microECs. In fact, our results suggest that certain MMPs, specifically MMP-7 and -13, significantly localized to MP over Sup fractions. Various secreted MMPs, including MMP-2, -1, -and -7, have been shown to bind to cell surfaces (Dumin et al., 2001, Puyraimond et al., 2001, Shiomi et al., 2005), and here we offer evidence that MPs bind exogenous MMP-2. We hypothesize that higher levels of certain MMPs in MP versus Sup fractions could be attributed to MPs binding MMPs, resulting in their simultaneous pull-down during MP isolation.

Our third aim was to study MP-regulation of MMP activities. We showed that MPs activated endogenous proMMP-2, a property not shared with the rest of EC-secreted factors. We also presented evidence linking MP-activation of MMP-2 with MMP-14. The role of MMP-14 in the activation of MMP-2 is well characterized (Hernandez-Barrantes et al., 2000, Stetler-Stevenson, 1999, Visse and Nagase, 2003, Werb, 1997, Worley et al., 2003). Here we obtained evidence that active MMP-14 expressed by MPs activates MMP-2. That microEC MPs express active MMP-14 further supports the argument that MPs are well suited for MMP-2 activation.

MPs also bound and activated exogenous MMP-2. As mentioned previously, we are interested in MPs in the context of the regulation of the perivascular niche. For this reason, we tested the effects of MPs on the MMP activity of MSC-CM. As co-residents with microECs in the perivascular niche, MSCs would contribute to the environment seen by MPs. We showed that MPs bound and activated proMMP-2 secreted by MSC. Since MSCs secrete high levels of TIMP-1 and TIMP-2 in addition to proMMP-2, these results suggest that MMP-2 is localized to the surface of MPs, converted to its active form, and is able to cleave substrate despite the presence of TIMPs. That MPs are able create a local environment where MMP-2 can be activated further supports the notion that microEC MPs act as focal centers of MMP activity.

We have also considered MMP inhibition. Non-MP factors secreted by microECs strongly inhibited exogenous MMPs, a trait not shared with MPs. Furthermore, EC-secreted factors included high levels of TIMP-1 and TIMP-2, which were not detected in MPs. We have previously shown that the MMP-inhibitory effects of microEC-secreted factors were due to TIMP-1 and TIMP-2 (Lozito and Tuan, 2010). Thus, the enrichment of MPs for MMP activities was not only due to the localization and activation of MMPs by MPs; MPs also lacked the TIMPs that characterize the remainder of the perivascular niche, thereby allowing MP-associated MMPs to actively cleave substrates. In contrast, the remaining EC-secreted factors lack MMP activity and inhibit high levels of exogenous MMPs with TIMP-1 and TIMP-2. By applying MMP inhibitor assays to MPs and the surrounding environment, we observed that MPs are conducive to MMP activity and the functional consequences of this interplay among TIMP and MMP localizations.

Finally, we showed that MPs alter the very matrix to which they are bound. Previous studies have shown that microparticles signal ECs to degrade matrix, but the degradation was not linked to the microparticles themselves (Taraboletti et al., 2002). Here we showed that MPs degraded bound fibronectin in a process that required both MMPs and binding interactions between the MPs and fibronectin.

In conclusion, with their exogenous MMP activities and their abilities to bind matrix, MPs are well suited for their postulated roles as centers for matrix remodeling. Outside of the MP-local microenvironment, MMPs are inhibited by TIMPs secreted by ECs and perivascular MSCs. In this study we demonstrated that MPs, through the creation of a local microenvironment conducive to MMP activation and activity, function as another tier of MMP-regulation, controlling *where* MMPs are allowed to act. Interestingly, MPs not only regulate the spatial activities of endogenous MMPs, but actually recruit exogenous MMPs from their surroundings, drawing them to locations where they are activated. Situated at the interface between matrix and the soluble compartment, these MP-associated MMPs occupy a unique and optimal position for functional modification of the perivascular extracellular matrix.

Supplementary Material

Refer to Web version on PubMed Central for supplementary material.

Acknowledgments

Contact grant sponsor: NIAMS IRP; Contact grant number: Z01AR41131.

References

Abid Hussein MN, Meesters EW, Osmanovic N, Romijn FP, Nieuwland R, Sturk A. Antigenic characterization of endothelial cell-derived microparticles and their detection ex vivo. J Thromb Haemost. 2003; 1:2434–2443. [PubMed: 14629480]

Ades EW, Candal FJ, Swerlick RA, George VG, Summers S, Bosse DC, Lawley TJ. HMEC-1: establishment of an immortalized human microvascular endothelial cell line. J Invest Dermatol. 1992; 99:683–690. [PubMed: 1361507]

Anderson HC. Matrix vesicles and calcification. Curr Rheumatol Rep. 2003; 5:222–226. [PubMed: 12744815]

Berckmans RJ, Neiuwland R, Boing AN, Romijn FP, Hack CE, Sturk A. Cell-derived microparticles circulate in healthy humans and support low grade thrombin generation. Thromb Haemost. 2001; 85:639–646. [PubMed: 11341498]

Brew K, Dinakarpandian D, Nagase H. Tissue inhibitors of metalloproteinases: evolution, structure and function. Biochim Biophys Acta. 2000; 1477:267–283. [PubMed: 10708863]

Combes V, Simon AC, Grau GE, Arnoux D, Camoin L, Sabatier F, Mutin M, Sanmarco M, Sampol J, Dignat-George F. In vitro generation of endothelial microparticles and possible prothrombotic activity in patients with lupus anticoagulant. J Clin Invest. 1999; 104:93–102. [PubMed: 10393703]

Crisan M, Yap S, Casteilla L, Chen CW, Corselli M, Park TS, Andriolo G, Sun B, Zheng B, Zhang L, Norotte C, Teng PN, Traas J, Schugar R, Deasy BM, Badylak S, Buhring HJ, Giacobino JP, Lazzari L, Huard J, Peault B. A perivascular origin for mesenchymal stem cells in multiple human organs. Cell Stem Cell. 2008; 3:301–313. [PubMed: 18786417]

Diamant M, Tushuizen ME, Sturk A, Nieuwland R. Cellular microparticles: new players in the field of vascular disease? Eur J Clin Invest. 2004; 34:392–401. [PubMed: 15200490]

Dolo V, Ginestra A, Ghersi G, Nagase H, Vittorelli ML. Human breast carcinoma cells cultured in the presence of serum shed membrane vesicles rich in gelatinolytic activities. J Submicrosc Cytol Pathol. 1994; 26:173–180. [PubMed: 8019942]

Dumin JA, Dickeson SK, Stricker TP, Bhattacharyya-Pakrasi M, Roby JD, Santoro SA, Parks WC. Pro-collagenase-1 (matrix metalloproteinase-1) binds the alpha(2)beta(1) integrin upon release from keratinocytes migrating on type I collagen. J Biol Chem. 2001; 276:29368–29374. [PubMed: 11359786]

Forman MB, Puett DW, Virmani R. Endothelial and myocardial injury during ischemia and reperfusion: pathogenesis and therapeutic implications. J Am Coll Cardiol. 1989; 13:450–459. [PubMed: 2643655]

Freyssinet JM. Cellular microparticles: what are they bad or good for? J Thromb Haemost. 2003; 1:1655–1662. [PubMed: 12871302]

Hamilton KK, Hattori R, Esmon CT, Sims PJ. Complement proteins C5b-9 induce vesiculation of the endothelial plasma membrane and expose catalytic surface for assembly of the prothrombinase enzyme complex. J Biol Chem. 1990; 265:3809–3814. [PubMed: 2105954]

Hernandez-Barrantes S, Toth M, Bernardo MM, Yurkova M, Gervasi DC, Raz Y, Sang QA, Fridman R. Binding of active (57 kDa) membrane type 1-matrix metalloproteinase (MT1-MMP) to tissue inhibitor of metalloproteinase (TIMP)-2 regulates MT1-MMP processing and pro-MMP-2 activation. J Biol Chem. 2000; 275:12080–12089. [PubMed: 10766841]

Hristov M, Erl W, Linder S, Weber PC. Apoptotic bodies from endothelial cells enhance the number and initiate the differentiation of human endothelial progenitor cells in vitro. Blood. 2004; 104:2761–2766. [PubMed: 15242875]

Ikejiri M, Bernardo MM, Bonfil RD, Toth M, Chang M, Fridman R, Mobashery S. Potent mechanism-based inhibitors for matrix metalloproteinases. J Biol Chem. 2005; 280:33992–34002. [PubMed: 16046398]

Jimenez JJ, Jy W, Mauro LM, Horstman LL, Ahn YS. Elevated endothelial microparticles in thrombotic thrombocytopenic purpura: findings from brain and renal microvascular cell culture and patients with active disease. Br J Haematol. 2001; 112:81–90. [PubMed: 11167788]

Lacroix R, Sabatier F, Mialhe A, Basire A, Pannell R, Borghi H, Robert S, Lamy E, Plawinski L, Camoin-Jau L, Gurewich V, Angles-Cano E, Dignat-George F. Activation of plasminogen into plasmin at the surface of endothelial microparticles: a mechanism that modulates angiogenic properties of endothelial progenitor cells in vitro. Blood. 2007; 110:2432–2439. [PubMed: 17606760]

Lozito TP, Tuan RS. Mesenchymal stem cells inhibit both endogenous and exogenous MMPs via secreted TIMPs. J Cell Physiol. 2010

Madri JA, Bell L, Marx M, Merwin JR, Basson C, Prinz C. Effects of soluble factors and extracellular matrix components on vascular cell behavior in vitro and in vivo: models of de-endothelialization and repair. J Cell Biochem. 1991; 45:123–130. [PubMed: 1711525]

Mallat Z, Benamer H, Hugel B, Benessiano J, Steg PG, Freyssinet JM, Tedgui A. Elevated levels of shed membrane microparticles with procoagulant potential in the peripheral circulating blood of patients with acute coronary syndromes. Circulation. 2000; 101:841–843. [PubMed: 10694520]

Minagar A, Jy W, Jimenez JJ, Sheremata WA, Mauro LM, Mao WW, Horstman LL, Ahn YS. Elevated plasma endothelial microparticles in multiple sclerosis. Neurology. 2001; 56:1319–1324. [PubMed: 11376181]

Oliver GW, Leferson JD, Stetler-Stevenson WG, Kleiner DE. Quantitative reverse zymography: analysis of picogram amounts of metalloproteinase inhibitors using gelatinase A and B reverse zymograms. Anal Biochem. 1997; 244:161–166. [PubMed: 9025922]

Puyraimond A, Fridman R, Lemesle M, Arbeille B, Menashi S. MMP-2 colocalizes with caveolae on the surface of endothelial cells. Exp Cell Res. 2001; 262:28–36. [PubMed: 11120602]

Ries C, Egea V, Karow M, Kolb H, Jochum M, Neth P. MMP-2, MT1-MMP, and TIMP-2 are essential for the invasive capacity of human mesenchymal stem cells: differential regulation by inflammatory cytokines. Blood. 2007; 109:4055–4063. [PubMed: 17197427]

Shi S, Gronthos S. Perivascular niche of postnatal mesenchymal stem cells in human bone marrow and dental pulp. J Bone Miner Res. 2003; 18:696–704. [PubMed: 12674330]

Shiomi T, Inoki I, Kataoka F, Ohtsuka T, Hashimoto G, Nemori R, Okada Y. Pericellular activation of proMMP-7 (promatrilysin-1) through interaction with CD151. Lab Invest. 2005; 85:1489–1506. [PubMed: 16200075]

Stetler-Stevenson WG. Matrix metalloproteinases in angiogenesis: a moving target for therapeutic intervention. J Clin Invest. 1999; 103:1237–1241. [PubMed: 10225966]

Taraboletti G, D'Ascenzo S, Borsotti P, Giavazzi R, Pavan A, Dolo V. Shedding of the matrix metalloproteinases MMP-2, MMP-9, and MT1-MMP as membrane vesicle-associated components by endothelial cells. Am J Pathol. 2002; 160:673–680. [PubMed: 11839588]

Visse R, Nagase H. Matrix metalloproteinases and tissue inhibitors of metalloproteinases: structure, function, and biochemistry. Circ Res. 2003; 92:827–839. [PubMed: 12730128]

Werb Z. ECM and cell surface proteolysis: regulating cellular ecology. Cell. 1997; 91:439–442. [PubMed: 9390552]

Worley JR, Thompkins PB, Lee MH, Hutton M, Soloway P, Edwards DR, Murphy G, Knauper V. Sequence motifs of tissue inhibitor of metalloproteinases 2 (TIMP-2) determining progelatinase A (proMMP-2) binding and activation by membrane-type metalloproteinase 1 (MT1-MMP). Biochem J. 2003; 372:799–809. [PubMed: 12630911]

Xu Y, Swerlick RA, Sepp N, Bosse D, Ades EW, Lawley TJ. Characterization of expression and modulation of cell adhesion molecules on an immortalized human dermal microvascular endothelial cell line (HMEC-1). J Invest Dermatol. 1994; 102:833–837. [PubMed: 7516395]

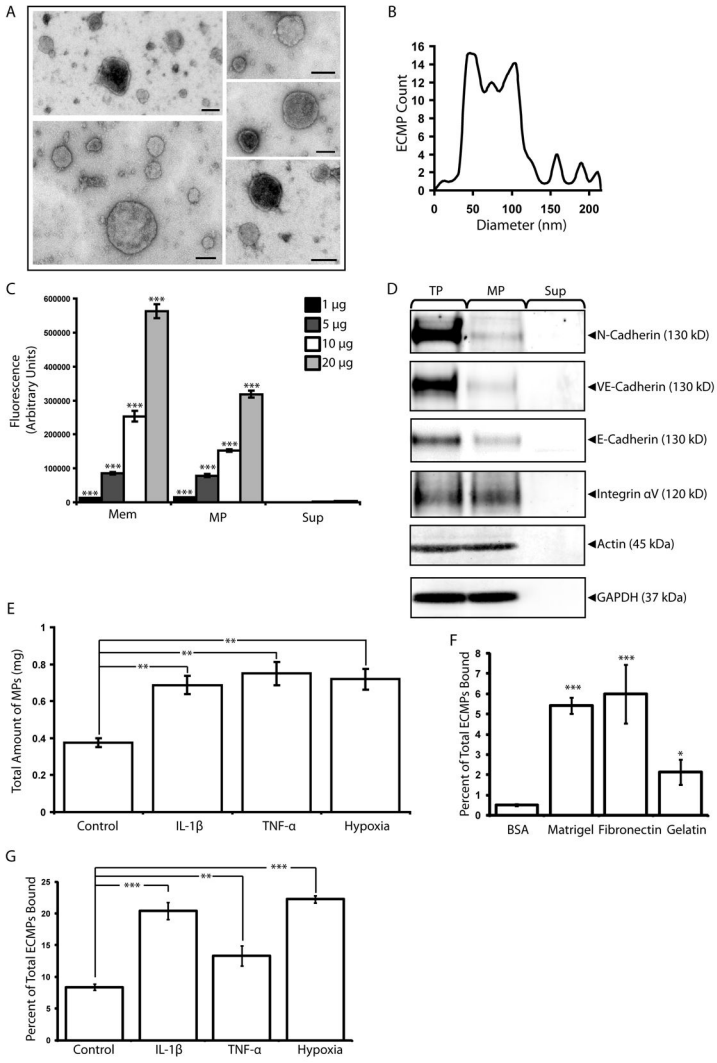

Figure 1.

MicroEC MPs are plasma membrane derived and bind to extracellular matrix substrates. (A) MPs isolated from microECs were observed by negative staining and transmission electron microscopy as intact membranous structures. (B) Size profile of isolated MPs. (C) Fluorescence photometry analysis of membranes (Mem), MP, and Sup samples (1, 5, 10, or 20 μg) isolated from DiO-labeled microECs. MPs and Mem samples were enriched for DiO. *** $p < 0.001$ compared to Sup values of corresponding protein amounts (D) Western blot analysis comparing localization of membrane proteins (N-cadherin, VE-cadherin, E-cadherin, Integrin α_V) among microEC total protein (TP), MPs, and Sup fractions. Blots of actin and GAPDH were included as loading controls. (E) Comparison of the amount of MPs produced under control conditions or in the presence of IL-1β, TNF-α, or hypoxia. ** $p < 0.01$ (F) DiO-labeled MPs bound to surfaces coated with Matrigel, fibronectin, or gelatin. * $p < 0.05$, *** $p < 0.001$ compared to BSA controls (G) Higher percentages of DiO-labeled MPs produced in the presence of IL-1β, TNF-α, or hypoxia bound fibronectin-coated surfaces than those produced under control conditions. ** $p < 0.01$ Results are means ± SD.

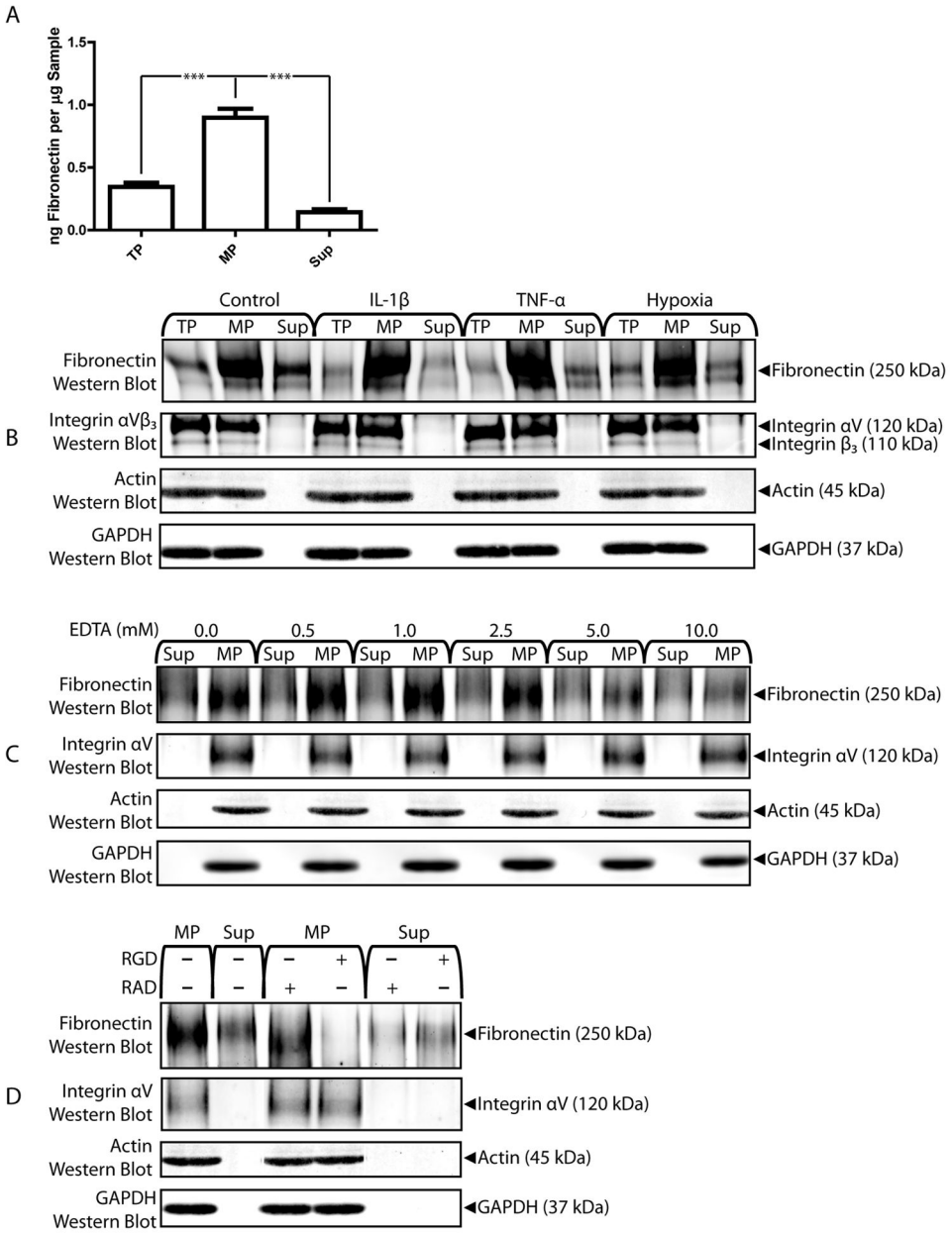

Figure 2.

MicroEC MPs bind endogenous fibronectin. (A) Fibronectin ELISA analysis of TP, MP, and Sup samples. *** $p < 0.001$ (B) Fibronectin and integrin $\alpha_V\beta_3$ western blots of TP, MP, and Sup samples collected from microECs cultured under control conditions or in the presence of IL-1β, TNF-α, or hypoxia. (C) High levels of EDTA during isolation reduced fibronectin associated with MPs. (D) Treatment with 2.5 mM RGD peptide, but not RAD, during isolation reduced fibronectin content of MPs. Results are means ± SD.

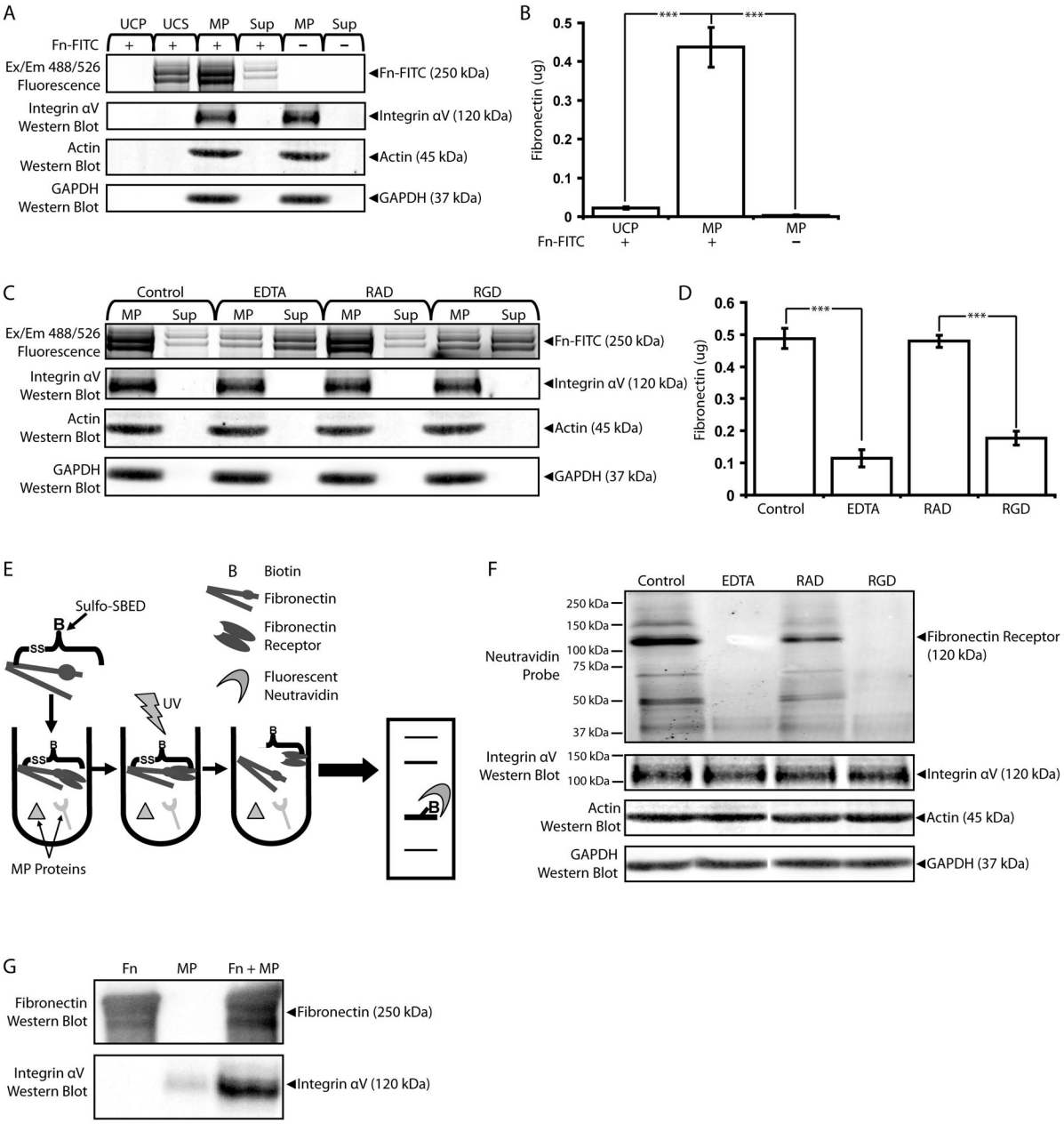

Figure 3.

MicroEC MPs bind exogenous fibronectin with integrin α_V. (A) FITC-labeled fibronectin (Fn-FITC) incubated with microEC-CM co-precipitated with MP samples. Ultracentrifugation pellets (UCP) and supernatants (UCS) collected from samples of Fn-FITC incubated without MPs were included as controls. All samples were analyzed with fluorescent scans of SDS-PAGE protein gels and integrin α_V western blots. (B) UCP and MPs incubated with or without Fn-FITC were also analyzed via fluorescence photometry for Fn-FITC content. *** $p < 0.001$ (C) Incubating EC-CM with Fn-FITC in the presence of 10 mM EDTA, or RGD (2.5 mM), but not RAD (2.5 mM), interfered with exogenous fibronectin localization to MP fractions. MP and Sup samples were analyzed for FN-FITC content via fluorescence scans of protein gels, and (D) MP samples were also analyzed by fluorescence photometry. *** $p < 0.001$ (E) “Bait and fish” method involving the biotin

transfer reagent sulfo-SBED in identifying fibronectin receptors. Exogenous fibronectin was pre-labeled with sulfo-SBED and incubated with MP proteins, including fibronectin receptors. Upon activation with UV light, the unreacted arm of sulfo-SBED was covalently crosslinked to fibronectin receptors. The disulfide-linkage between fibronectin and the fibronectin receptors was cleaved, and the samples were subjected to SDS-PAGE. Upon transfer to a PVDF membrane, fibronectin receptors were detected with fluorescent neutravidin probes. (F) 120 kDa fibronectin receptors were detected in MP samples crosslinked with sulfo-SBED-labeled fibronectin. Bands corresponding to fibronectin receptors were also detected in integrin α_V western blots. Biotin was not transferred to fibronectin receptors in the presence of EDTA (10mM), or RGD (2.5 mM). (G) Fibronectin and integrin α_V western blot analyses of samples of sulfo-SBED-labeled fibronectin, MP protein alone, or sulfo-SBED fibronectin incubated with MP proteins precipitated by monomeric avidin. Results are means ± SD.

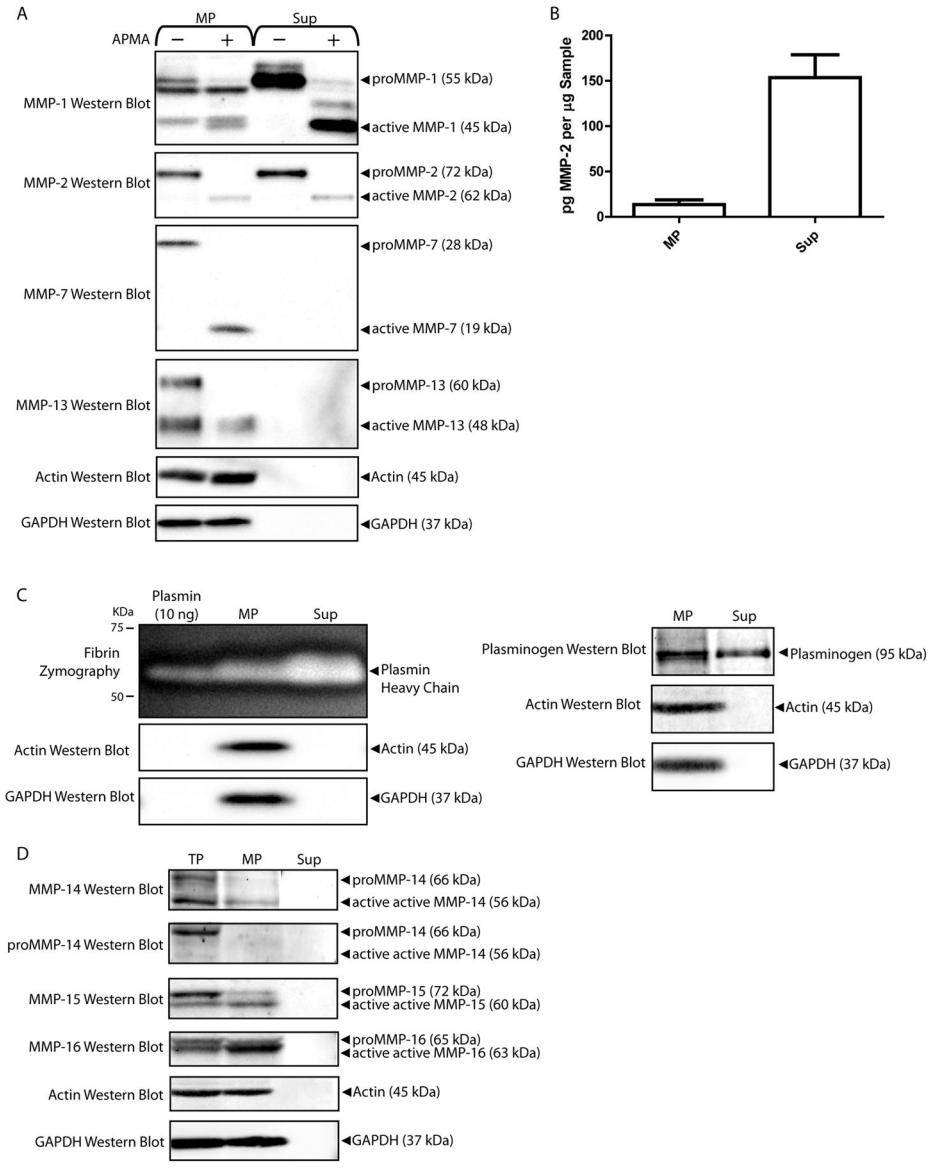

Figure 4.

MPs contain multiple MMPs. (A) Western blot detection of MMP-2, MMP-13, MMP-7, MMP-1 and plasminogen in MP and Sup protein samples treated with APMA or vehicle control. (B) MMP-2 ELISA analysis of MP and Sup samples. *** $p < 0.001$ (C) Fibrin zymography of and plasminogen western blot of MP and Sup fractions. Samples of plasmin (10 ng) were included in fibrin zymograms as positive controls. (D) Samples of microEC TP, MP, and Sup were analyzed by MMP-14, MMP-15, and MMP-16 western blots. Results are means ± SD.

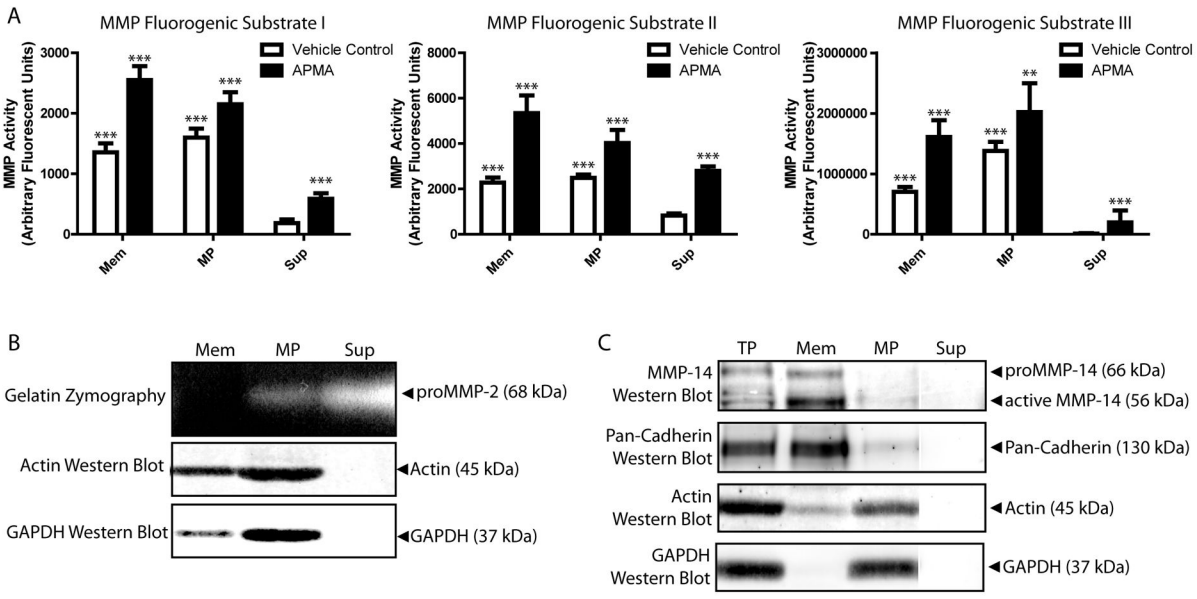

Figure 5.

MMPs are enriched in MMP- activities. (A) MicroEC Mem and MP samples, either treated with APMA or vehicle control, exhibited higher MMP activities than Sup samples in assays using 3 different fluorogenic MMP substrates. Asterisks above APMA values denote comparisons to corresponding vehicle control samples, while asterisks above Mem and MP vehicle control samples denote comparisons to Sup vehicle control samples. ** $p < 0.01$, *** $p < 0.001$ Results are means ± SD. (B) Gelatin zymography analysis of Mem, MP, and Sup fractions. (C) MMP-14 and pan-cadherin western blot analysis of microEC TP, Mem, MP, and Sup fractions.

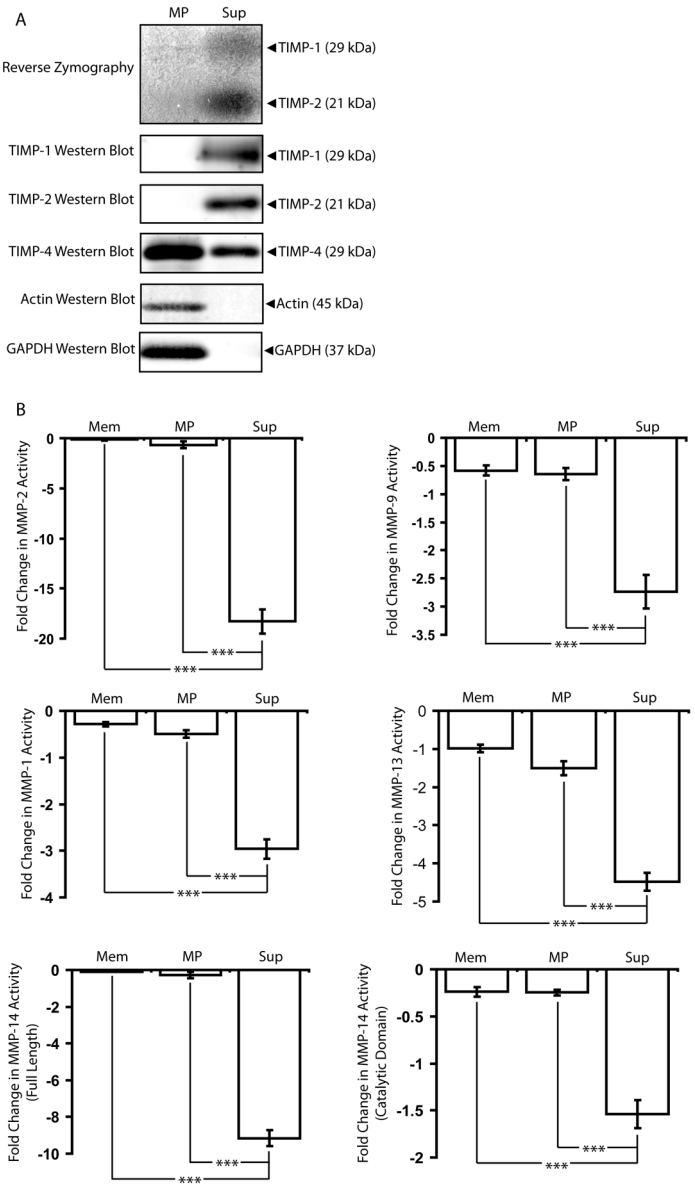

Figure 6.

MPs lack the MMP-inhibition activity found associated with the rest of microEC-secreted factors. (A) Samples of microEC MP and Sup fractions were analyzed via reverse zymography and by TIMP-1, TIMP-2, and TIMP-4 western blots. (B) Sup samples inhibited MMP-2, MMP-9, MMP-1, MMP-13, and MMP-14 activities more than Mem and MP samples. *** $p < 0.001$ Results are means ± SD.

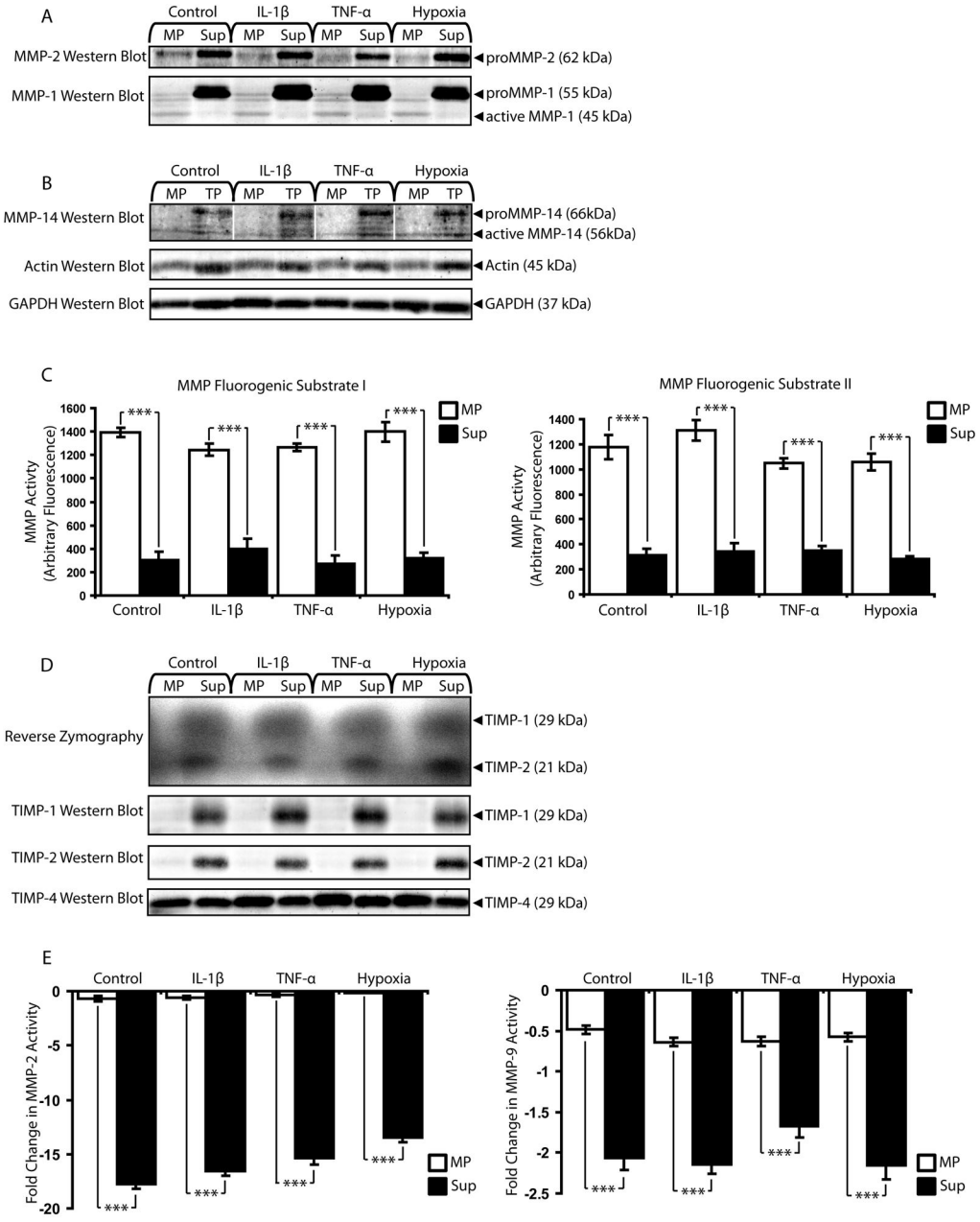

Figure 7.

MPs remain functional units of MMP activity in pathological conditions simulated in vitro with cytokines and hypoxia. (A) MMP-2 and MMP-1 western blot of MP and Sup fractions collected from microECs cultured under simulated pathological conditions (exposure to IL-1β, TNF-α, or hypoxia). (B) MMP-14 western blot of microEC MP and TP samples from control and pathological conditions. (C) MMP activity assays with MMP substrates I and II. ***$p < 0.001$ (D) Reverse zymography and TIMP-1, 2, and 4 western blots of MP and Sup produced in the presence of IL-1β, TNF-α, or hypoxia. (E) MMP-2 and MMP-9 inhibitor assays. ***$p < 0.001$ Results are means ± SD.

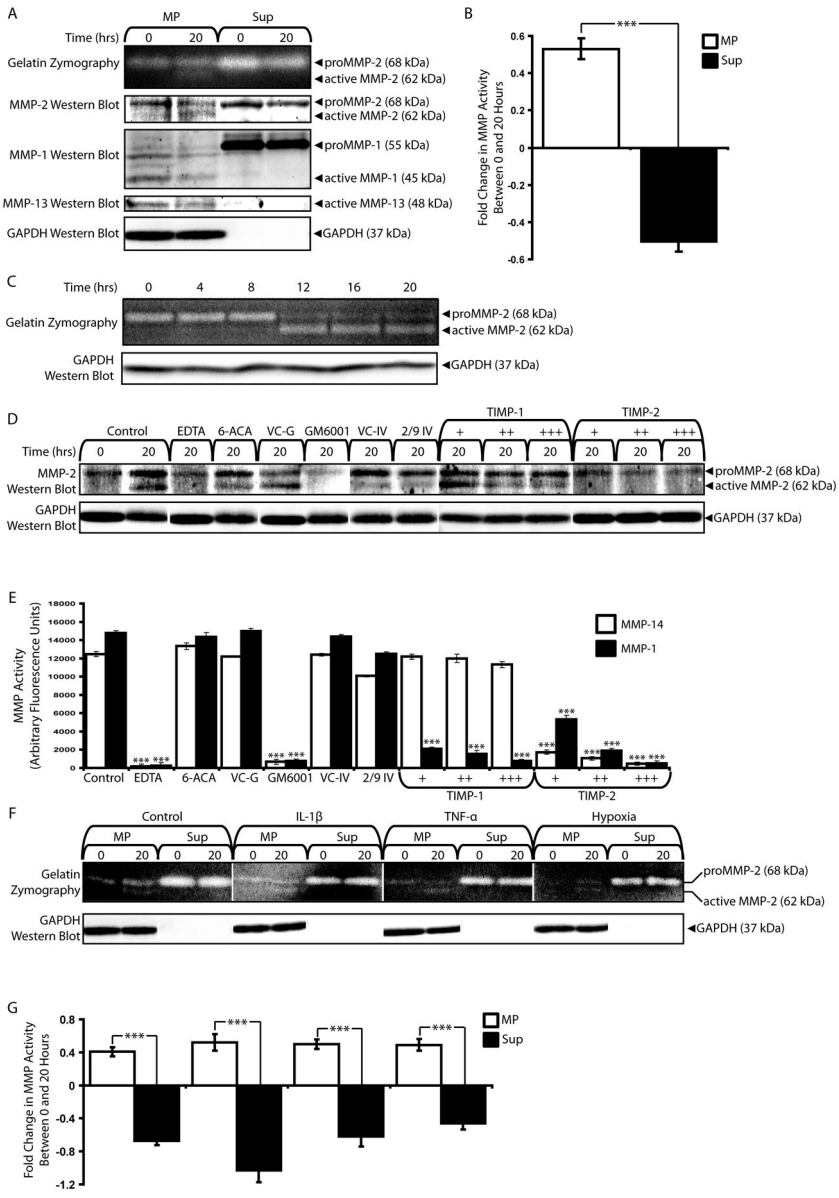

Figure 8.

MPs activate endogenous MMP-2. (A) Gelatin zymography and MMP-2, -1, and -13 western blot analyses of MP and Sup fractions incubated for 0 or 20 hours at 37°C. Active MMP-2 was detected in incubated MP samples. (B) MMP activities of MP, but not Sup, samples increased after 20 hours of incubation at 37°C. *** $p < 0.001$ (C) Time-dependence of MMP-2 activation in MP fractions over 20 hours. (D) MMP-2 western blot of MP samples incubated for 20 hours under control conditions or in the presence of inhibitors: 10 mM EDTA, 10 mM 6-aminocaproic acid (6-ACA), GM6001 vehicle control (VC-G), 20 μM GM6001, MMP-2/9 Inhibitor IV vehicle control (VC-IV), 2 μM MMP-2/9 inhibitor IV (2/9 IV), TIMP-1 (1 nM (+), 5 nM (++), 10 nM (+++)) or TIMP-2 (+, ++, +++). (E). MMP-14 and MMP-1 activity assays of inhibitor effects. *** $p < 0.001$ (F) Gelatin zymography and (G) MMP activity assays comparing MPs and Sup isolated from microECs treated with IL-1β, TNF-α, or hypoxia following incubation for 0 or 20 at 37°C. *** $p < 0.001$ Results are means ± SD.

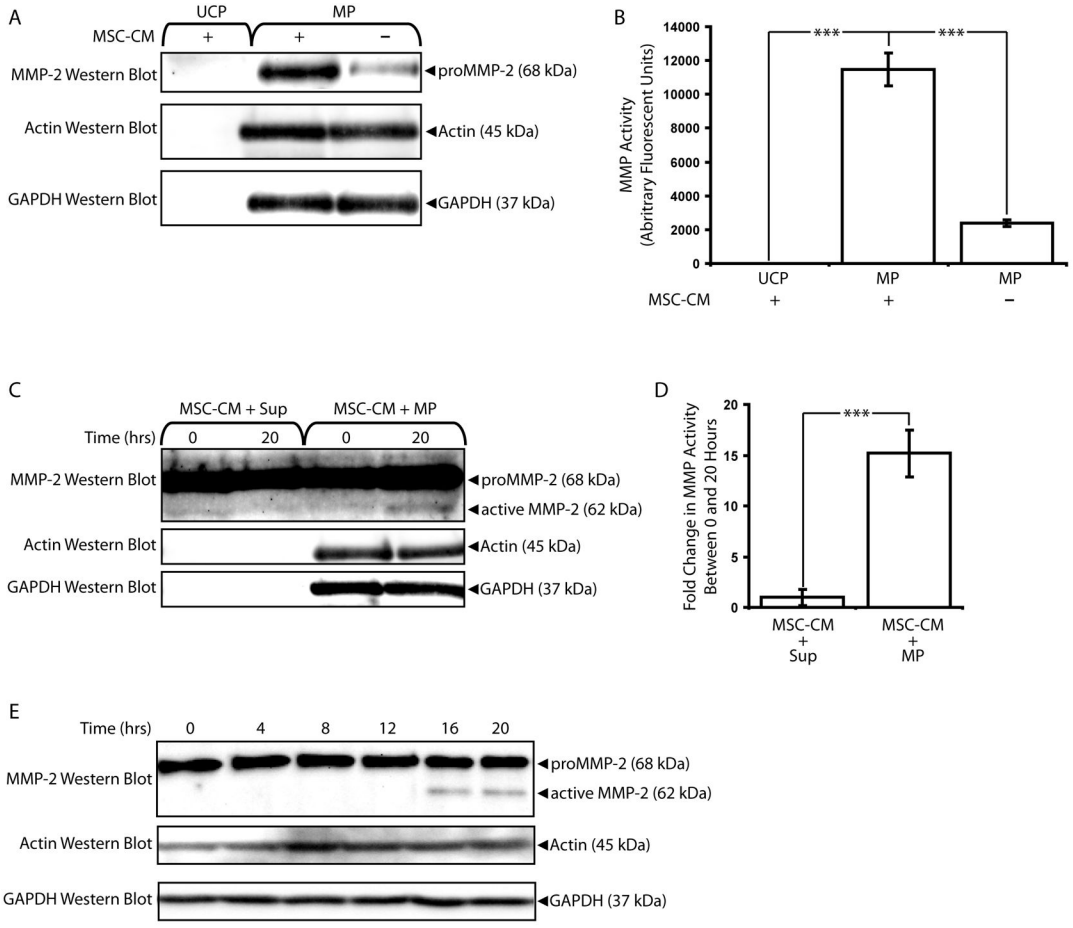

Figure 9.

MPs bind and activate exogenous MMP-2. (A) MMP-2 western blot analysis of MP fractions pre-incubated with or without MSC-CM. Ultracentrifugation pellets (UCP) collected from samples of MSC-CM incubated without MPs were included as negative controls, and blots of actin and GAPDH served as loading controls. MSC-secreted MMP-2 localized to MP fractions. (B) UCP and MPs incubated with or without MSC-CM were analyzed via MMP activity assays. *** $p < 0.001$ (C) MSC-CM samples were incubated with MP or Sup fractions for 0 or 20 hours and analyzed via MMP-2 western blots. Active MMP-2 was detected primarily in MSC-CM samples incubated with MPs. (D) MSC-CM samples incubated with MPs exhibited higher increases in MMP activity than those incubated with Sup fractions. *** $p < 0.001$ (E) Time-dependence of MMP-2 activation in MSC-CM samples incubated with MP fractions over 20 hours. Results are means ± SD.

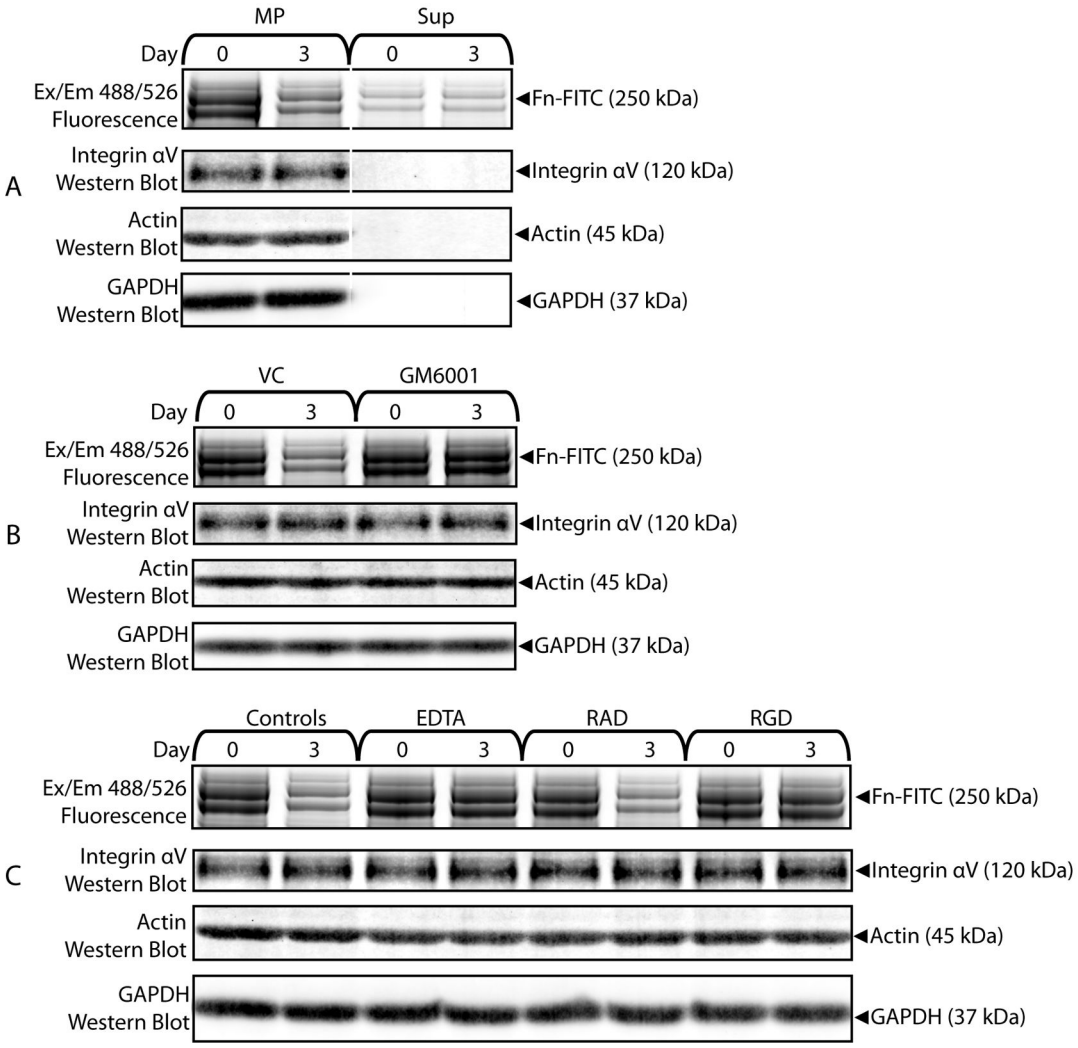

Figure 10.

MPs degrade bound matrix molecules with MMPs. (A) Fn-FITC samples co-isolated with MP or Sup were incubated for 0 or 3 days and analyzed with fluorescent scans of SDS-PAGE protein gels and integrin α_V western blots. Fn-FITC incubated with MPs was degraded. (B) Samples of Fn-FITC co-precipitated with MPs and incubated with GM6001 (20 μM) exhibited less degradation than samples incubated with vehicle controls (VC). (C) EDTA (10 mM) and RGD (2.5 mM), but not RAD (2.5 mM), interfered with degradation of Fn-FITC by MPs.